

# Diffuse TeV emission from the Cygnus region

References:

“Discovery of TeV gamma-ray emission from the Cygnus region of the Galaxy”

Abdo et al., astro-ph/0611691

“Dissecting the Cygnus region with TeV gamma rays and neutrinos”

Beacom & Kistler, astro-ph/0701751

Masaki Mori

ICRR CANGAROO group Internal seminar, February 1, 2007

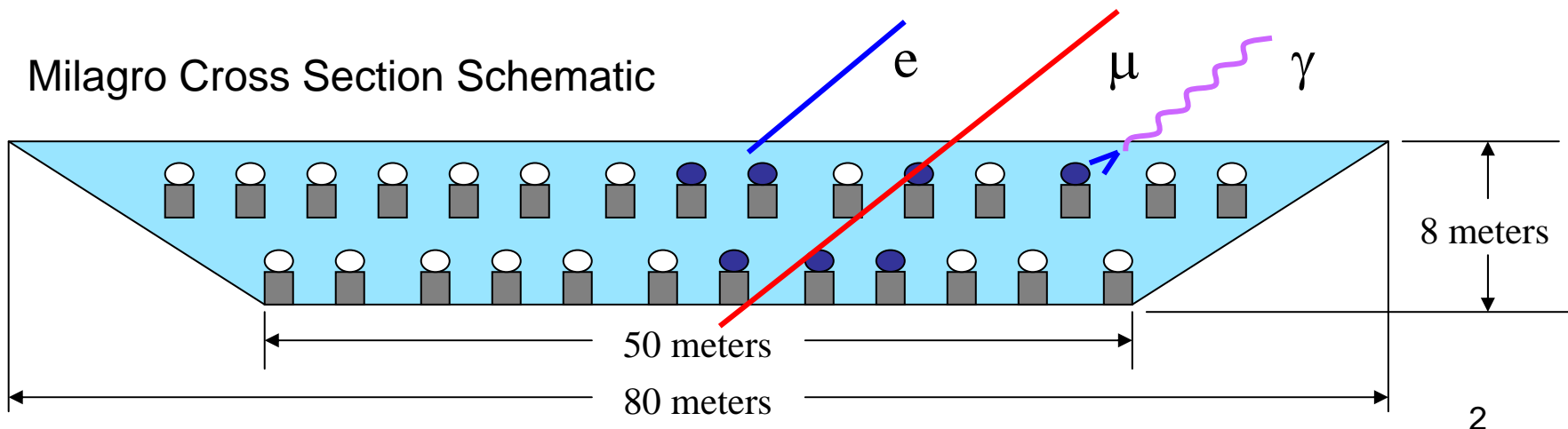
# Milagro

- A Water Cherenkov detector.
- Reconstruct shower direction to 0.3-0.7° from the timing shower front.
- Reject background by detecting penetrating component of hadronic showers
- Field of view is ~2 sr
- Duty factor ~95%
- Trigger rate ~1700 Hz (6 Mbytes/sec)

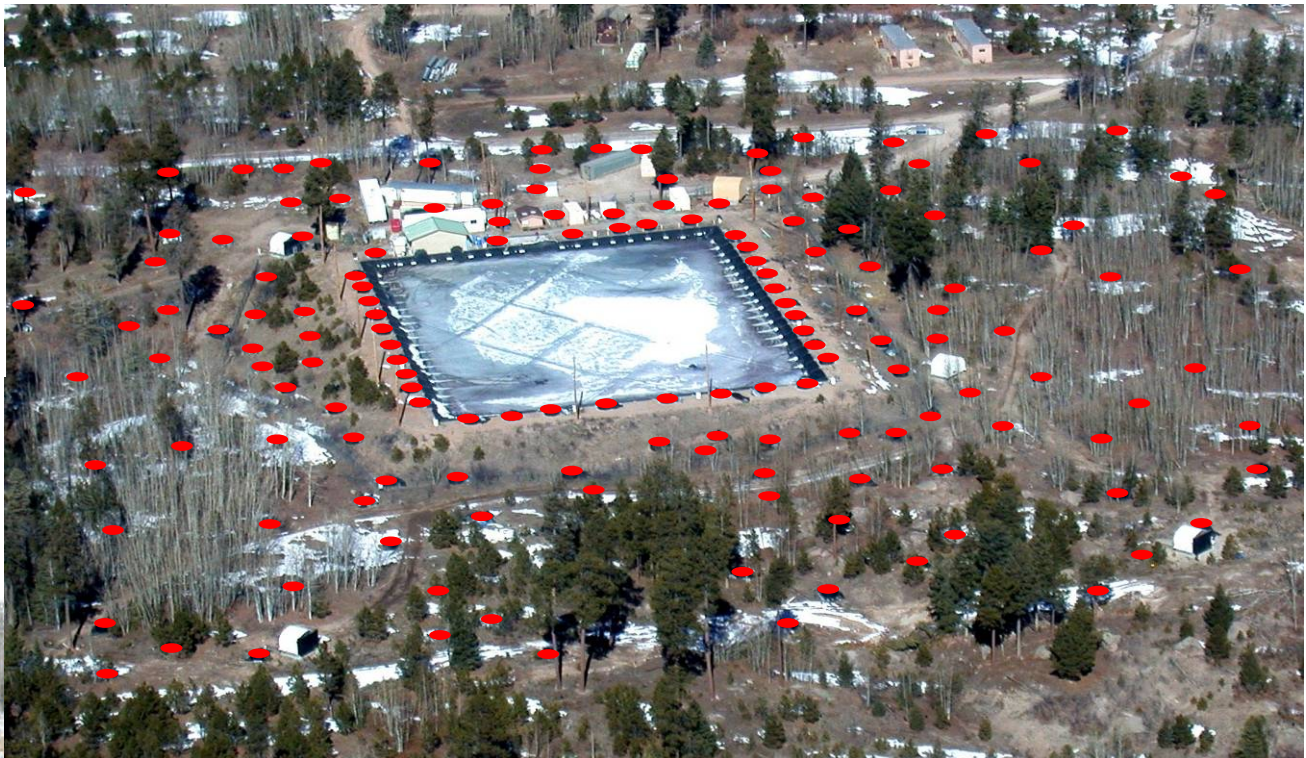
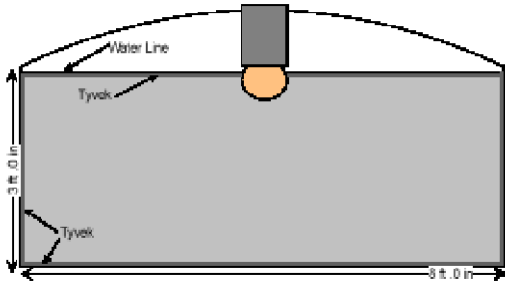
Los Alamos, NM,  
2650m a.s.l.



Milagro Cross Section Schematic



# Milagro with outriggers



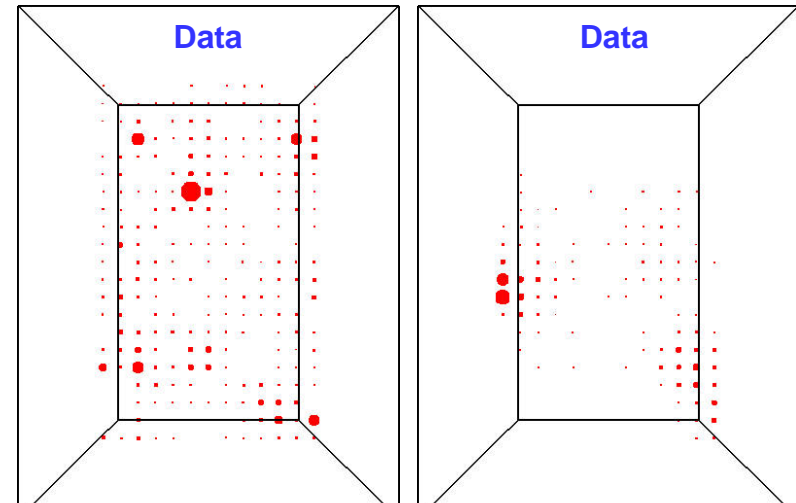
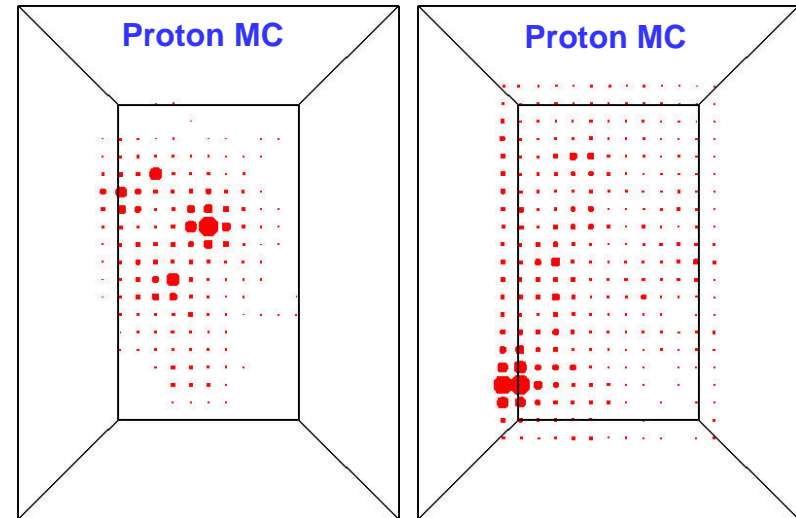
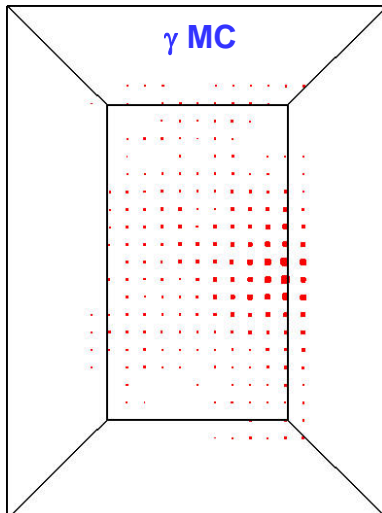
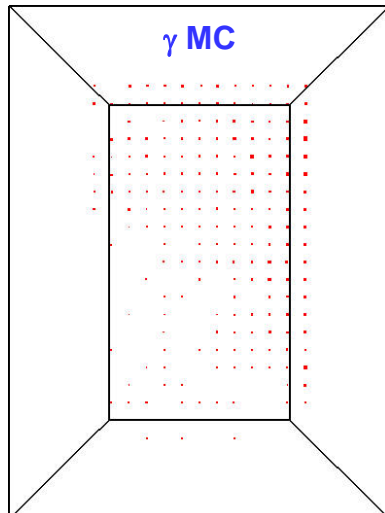
175 Outrigger tanks (Tyvek lined – water filled)  
2.4m diameter, 1m deep  
34,000 m<sup>2</sup> enclosed area  
Completed in May 2003

Angular resolution: 0.5deg (with outriggers) / 0.75deg (without)

# Background rejection in Milagro

Hadronic showers contain penetrating component:  $\mu$ 's & hadrons

- Cosmic-ray showers lead to clumpier bottom layer hit distributions
- Gamma-ray showers give smooth hit distributions



# Background rejection (cont'd)

- Parameterize “clumpiness” of the bottom layer hits

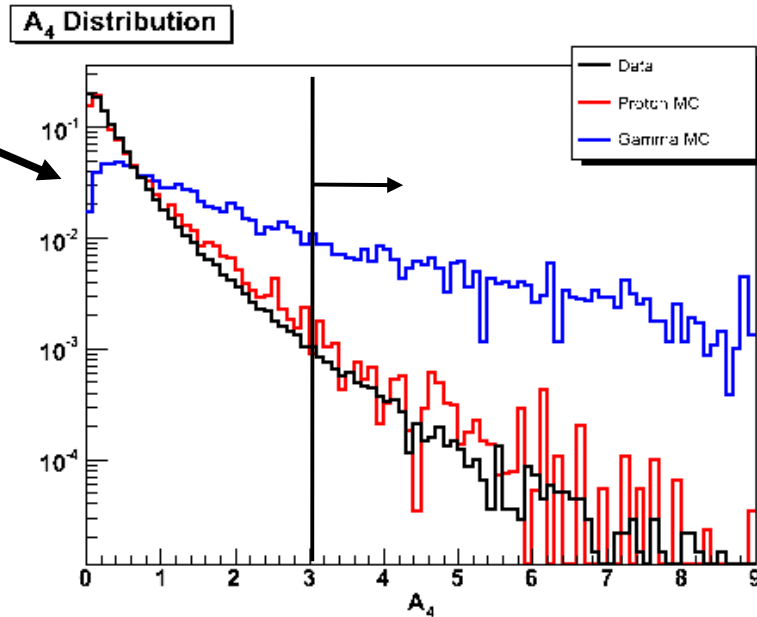
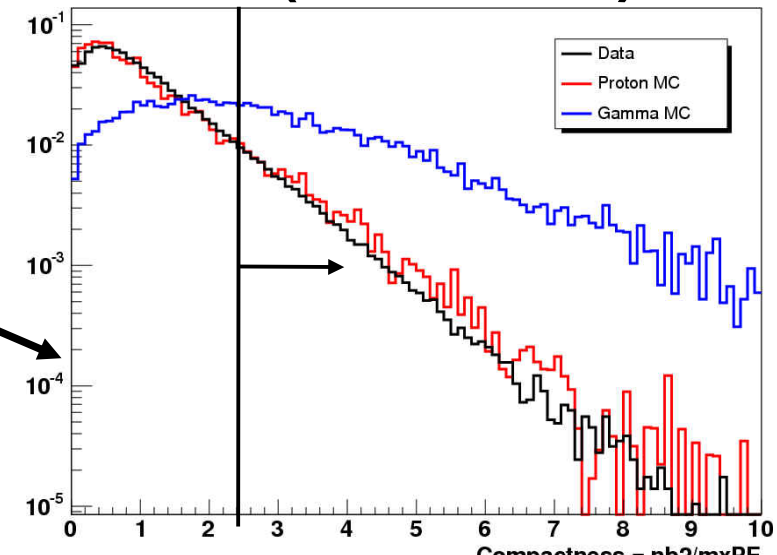
– Compactness  $C = \frac{nb2}{mxPE}$

- Require  $C > 2.5$
- 50% gammas & 10% hadrons
- Sensitivity improved by 1.6

$$A_4 = \frac{(fTop + fOut) * nFit}{mxPE}$$

- Require  $A_4 > 3.0$
- 20% gammas & 1% hadrons
- Sensitivity further improved by 1.4

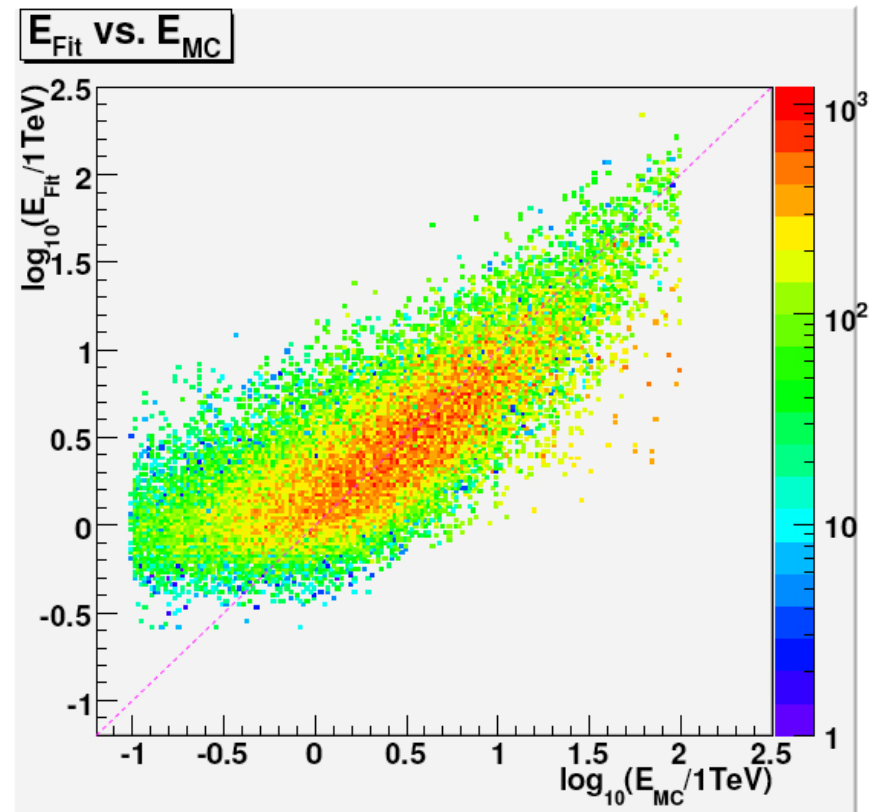
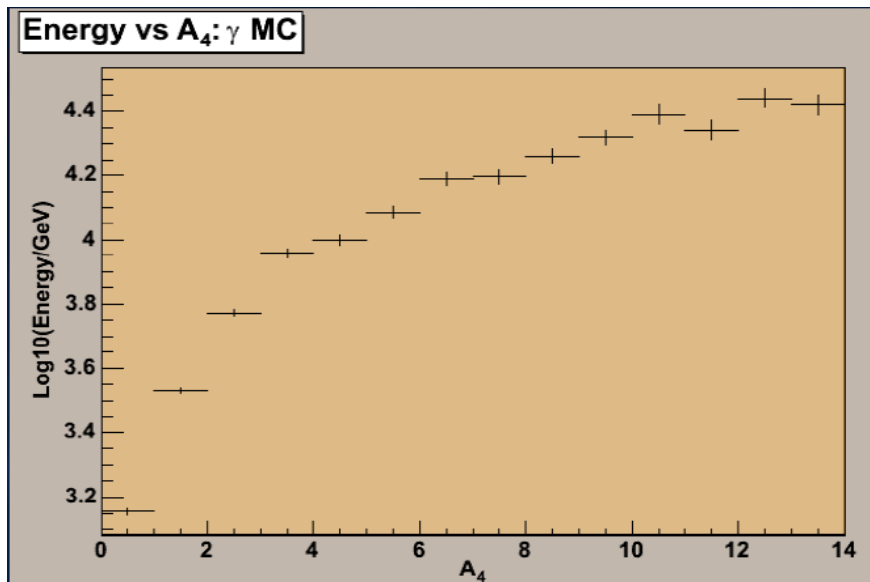
mxPE:	maximum # PEs in bottom layer PMT
nb2:	# bottom layer PMTs with 2 PEs or more
fTop:	# fraction of hit PMTs in Top layer
fOut:	# fraction of hit PMTs in Outriggers
nFit:	# PMTs used in the angle reconstruction



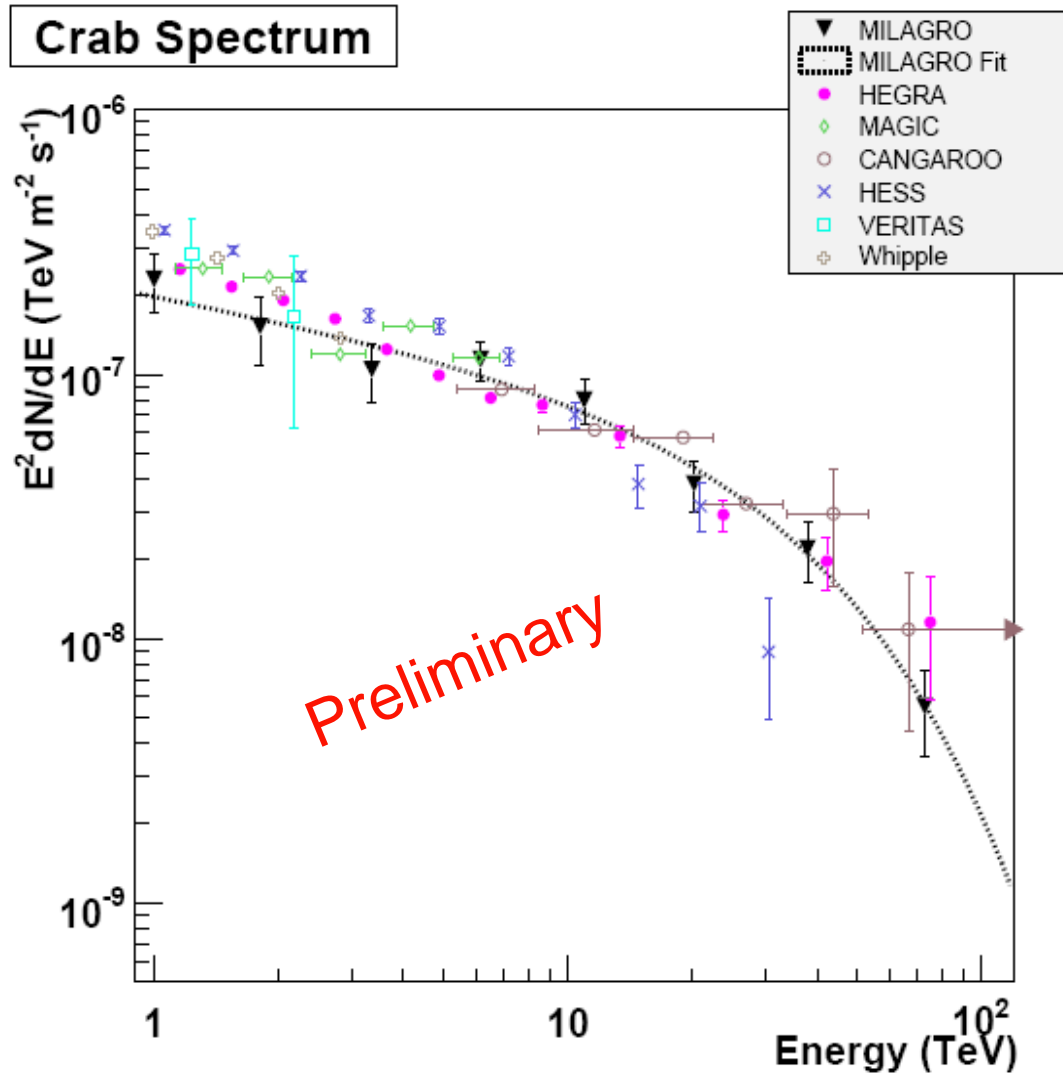
# Spectral determination

$A_4$  is related to energy  
2-20 TeV useful range

Parameterization of events



# Crab spectrum



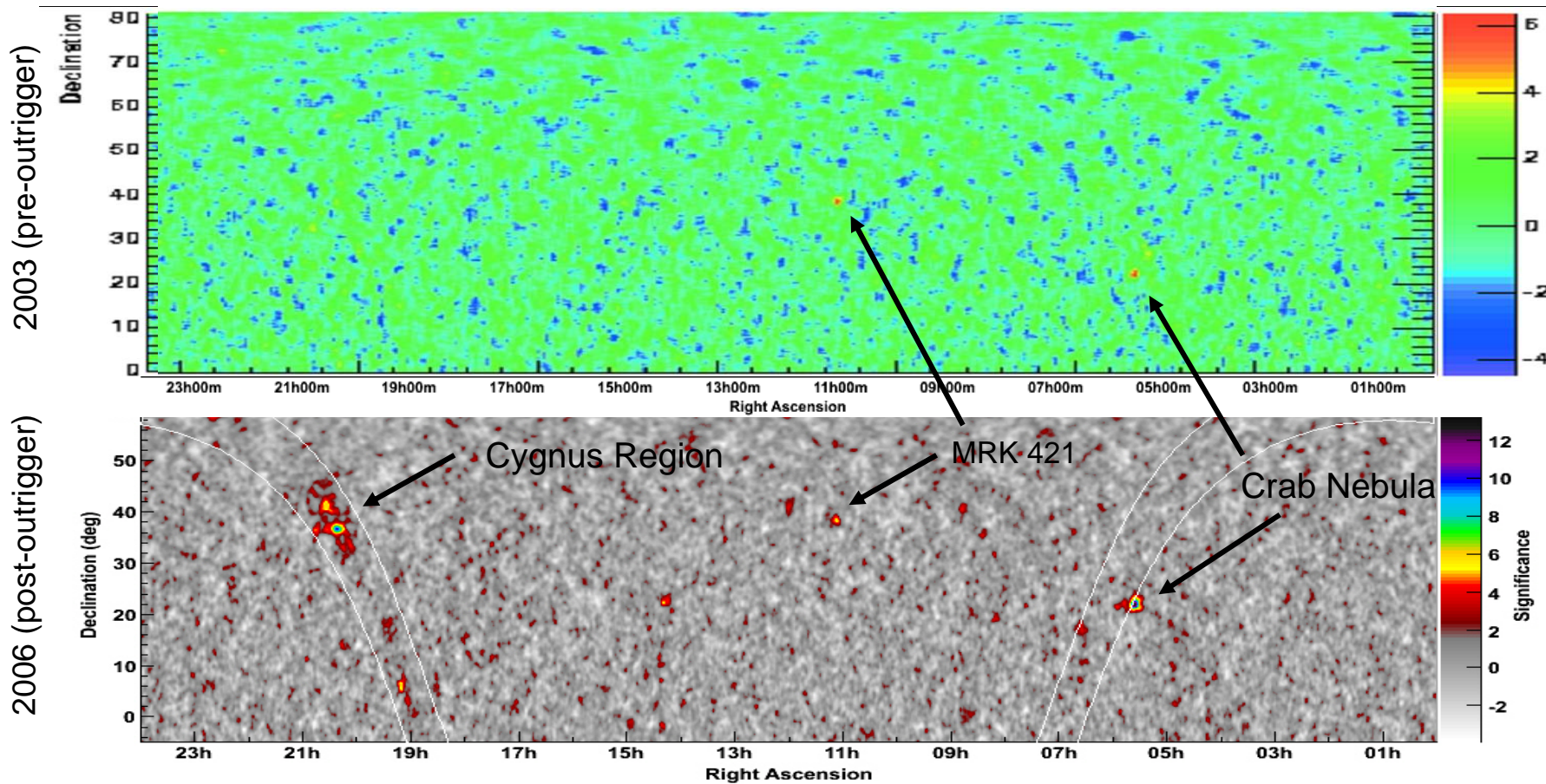
Exponential cut off energy is  
 $E_c = 31.0 \text{ TeV}$  (w/large error  
bars)

# Notes in the paper

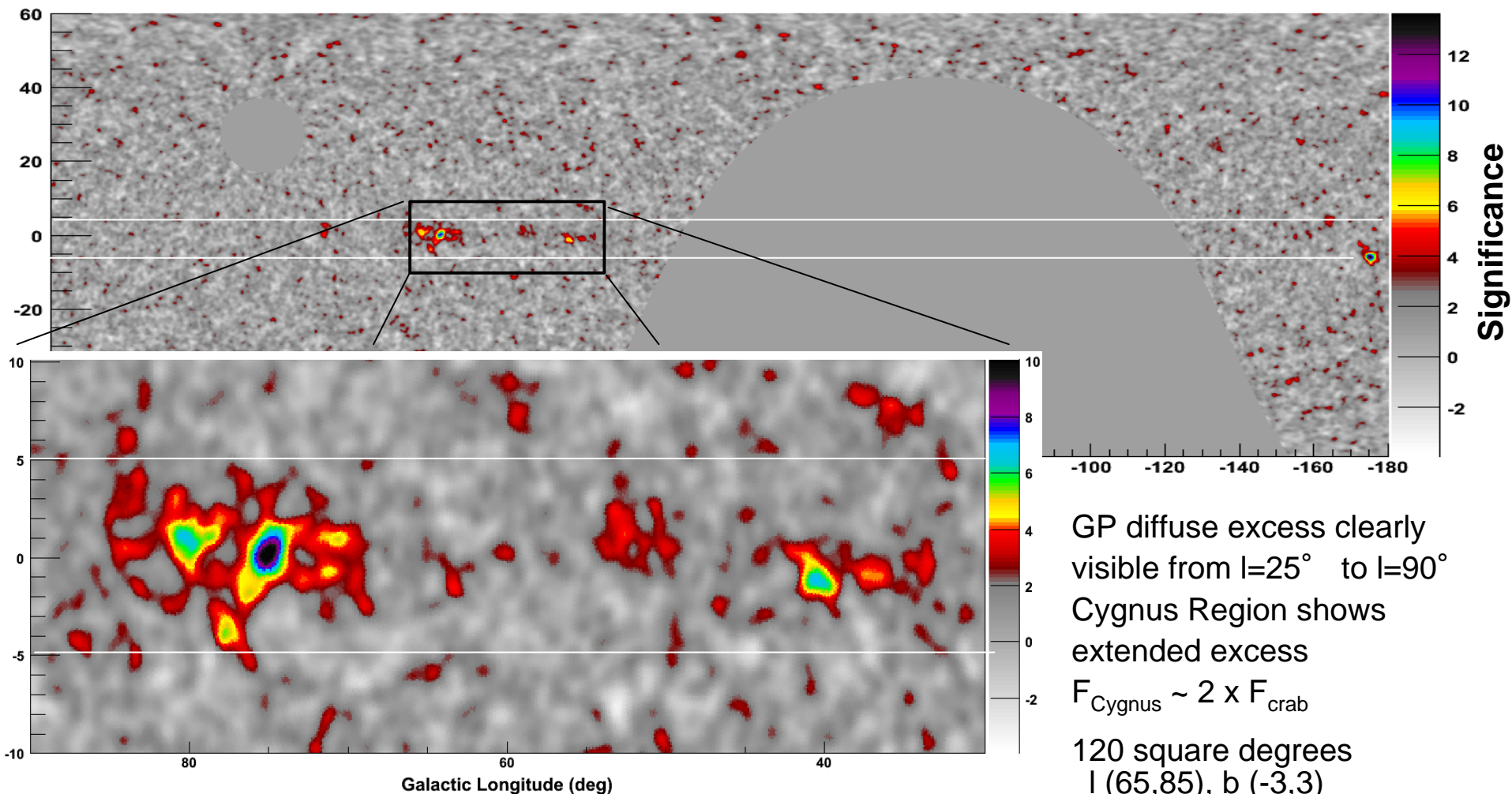
The dependence of the derived source flux on the spectrum is minimized when it is quoted at the median detected energy, which is  $\sim 12$  TeV for typical gamma-ray power law spectra and the weighted analysis using  $A_4$ . A change in the assumed source differential photon spectral index from -2.4 to -2.8 changes the quoted flux at 12 TeV by < 10%.

However, the Milagro trigger rate as determined from simulations of protons and helium using the flux from direct measurements (Haino *et al.* 2004 & Asakimori *et al.* 1998) is underpredicted, so a systematic error of 30% is given to the gamma-ray fluxes quoted here.

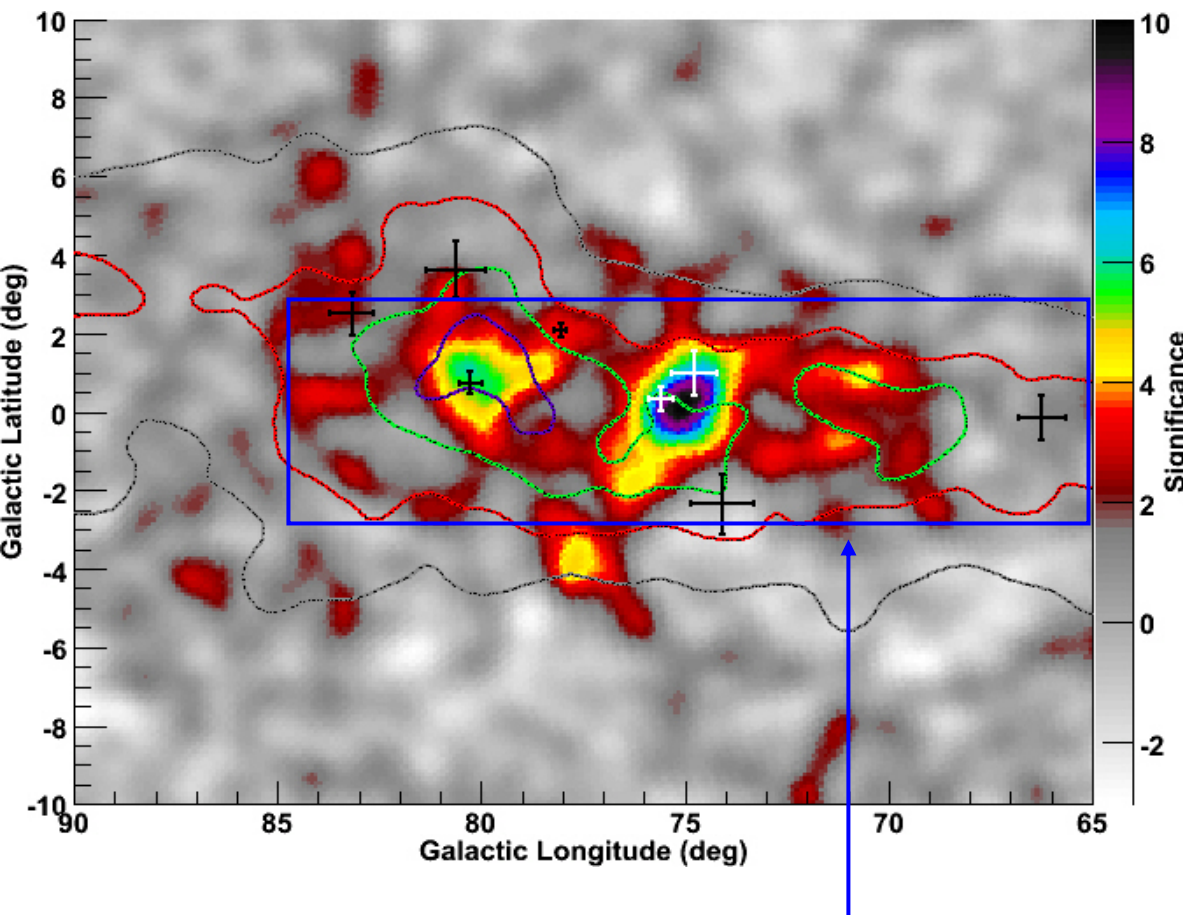
# Milagro sky survey



# The Galactic plane



# The Cygnus region



- Contours are GALPROP pion model
- Crosses are EGRET (unidentified) sources
- TeV/matter correlation good  
Chance noncorrelation  $1.5 \times 10^{-6}$
- Brightest TeV Region
  - **MGRO J2019+37**
  - $\sim 0.5$  Crab @ 12 TeV
  - Extent =  $0.32 \pm 0.12$  deg.
  - Coincident with 2 EGRET sources (unID)
    - PWN G75.2 + 0.1
    - Blazar (B2013+370)
  - *Energy Analysis in progress*

Flux @ 12.5 TeV =  $E^2 dN/dE = (4.18 \pm 0.52_{\text{stat}} \pm 1.26_{\text{sys}}) \times 10^{-10} \text{ TeV cm}^{-2} \text{ s}^{-1} \text{ sr}^{-1}$   
 (excluding new source & assuming  $E^{-2.6}$ )  
 ~3.5 Crab in 180 sq. degree region

# MGRO J2019+37

- Position:  $(\alpha, \delta) = (304.83 \pm 0.14 \pm 0.3, 36.83 \pm 0.08 \pm 0.25)$  deg
- Source size:  $0.32 \pm 0.12$  deg (high energy events [0.35deg ang.res.] only)
- Flux:  $E^2 dN/dE = (3.49 \pm 0.47 \pm 1.05) \times 10^{-12}$  TeV cm $^{-2}$ s $^{-1}$  at the median detected energy of 12TeV (assuming  $E^{-2.6}$ )

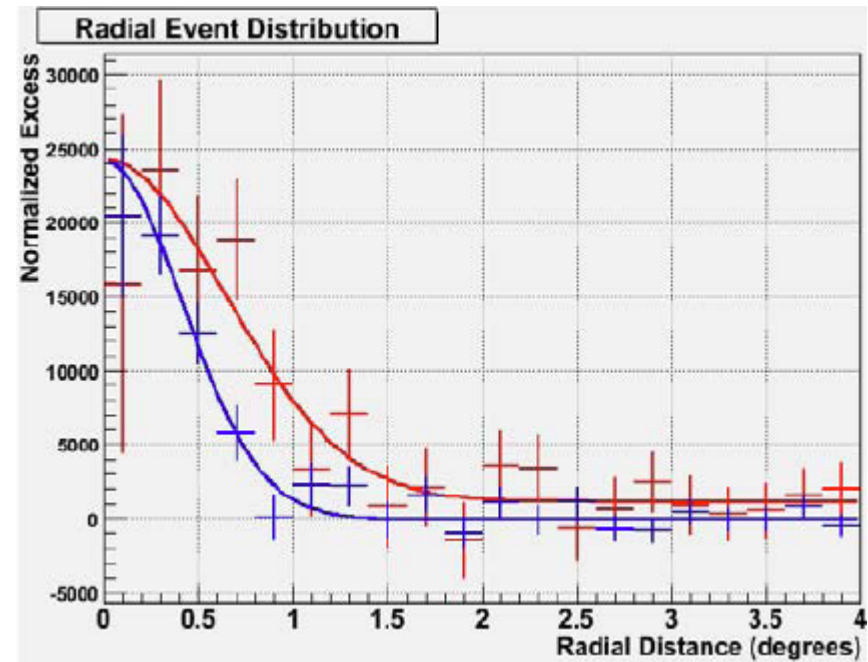
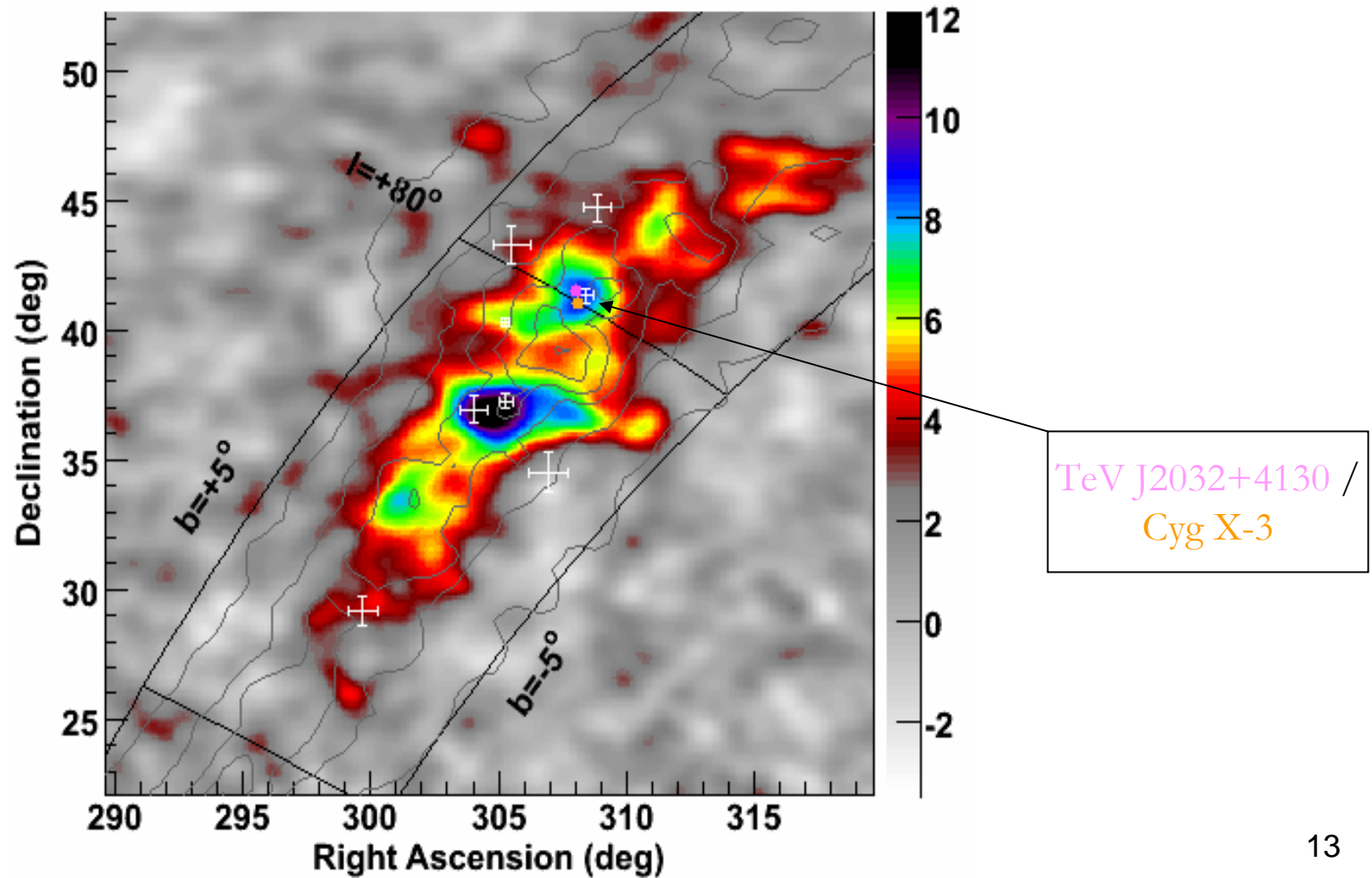
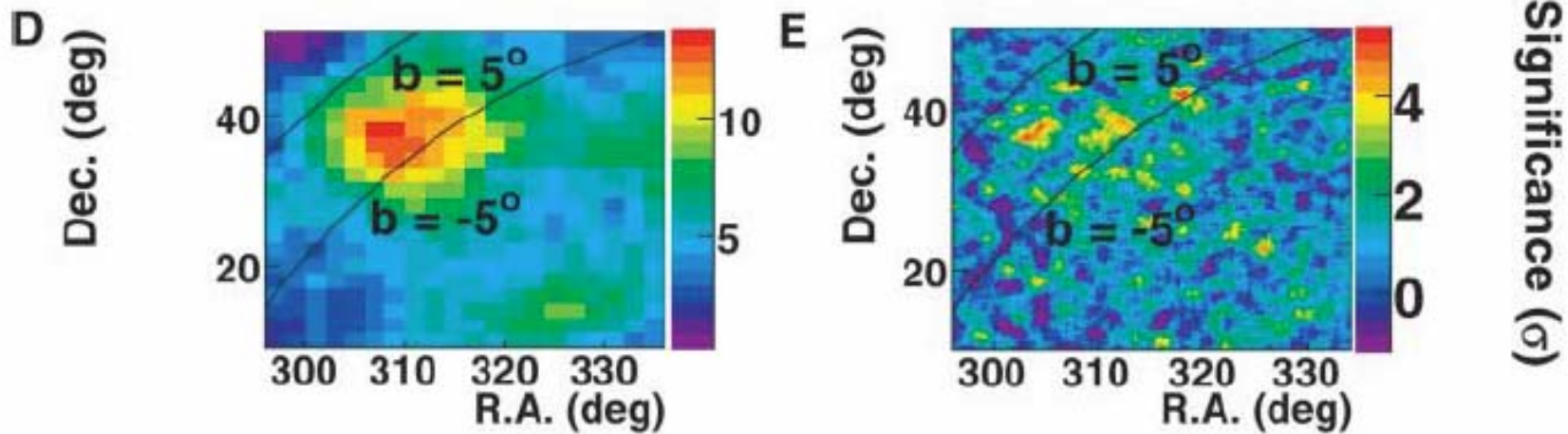


Figure 4 Radial profile of events from the direction of the Crab (blue) and from MGRO J2019+37 (red). Only events with large number of photomultiplier tube hits and outrigger information are shown due to their better angular resolution.

# Cygnus region

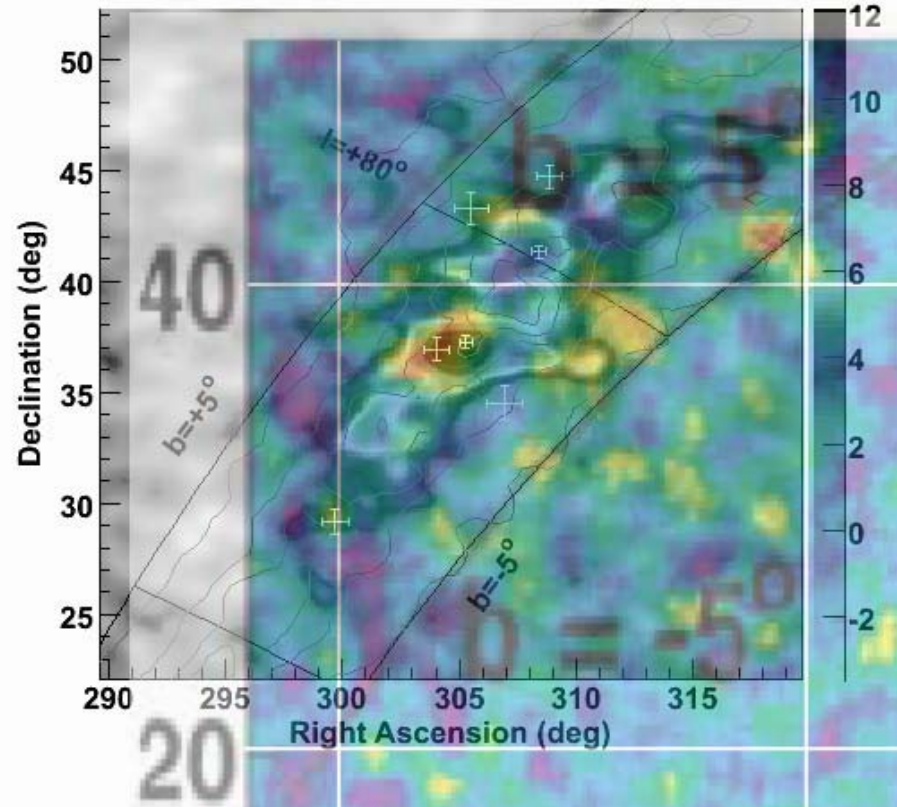
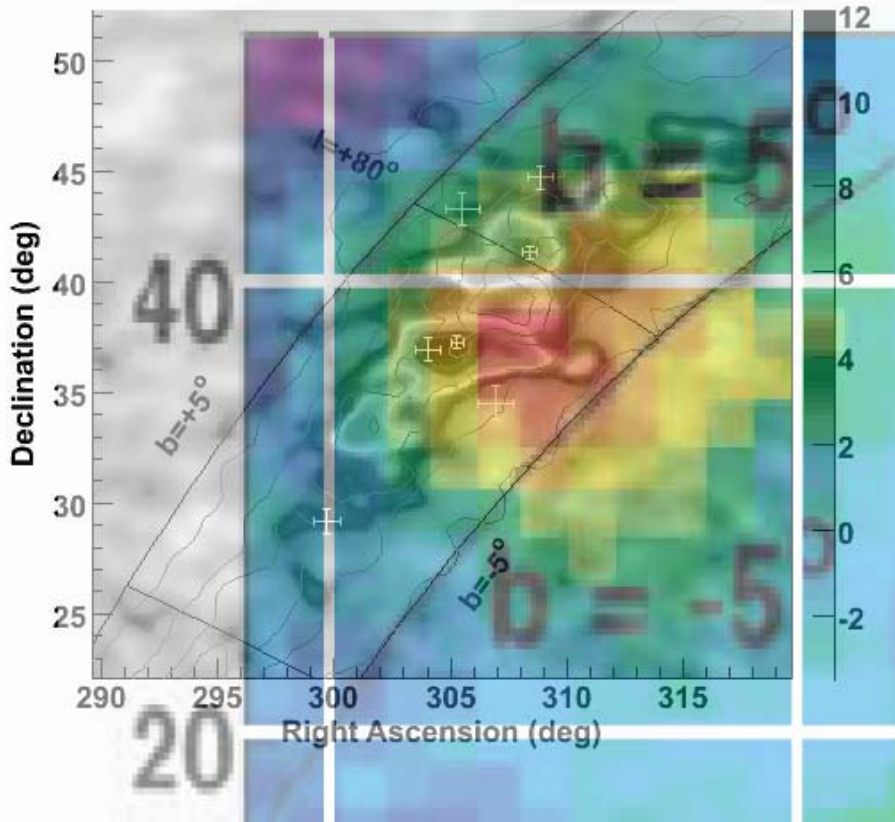


# Cygnus region: Tibet



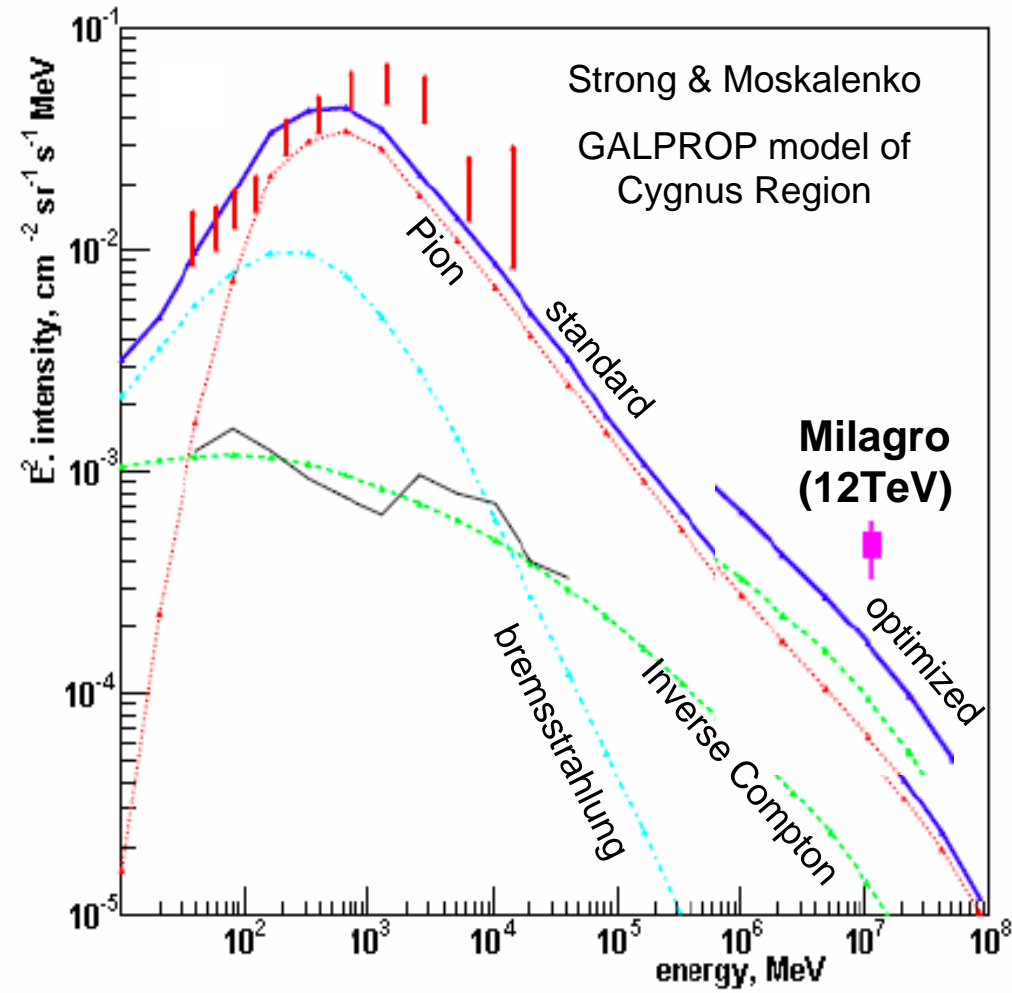
(D) and (E) show significance maps of the Cygnus region [pixels in radius of  $0.9^\circ$  and sampled over a square grid of side width  $0.25^\circ$  for (E)] for data from 1997 to 2005. The vertical color bin widths are  $0.69$  SD and  $0.42$  SD for significance in (D) and (E), respectively. Two thin curves in (D) and (E) stand for the Galactic parallel  $b = \pm 5^\circ$ . Small-scale anisotropies (E) superposed onto the large-scale anisotropy hint at the extended gamma-ray emission.

# Cygnus region: Milagro & Tibet



MILAGRO: A. Abdo, Santa Fe Workshop, May 2006  
Tibet: Amenomori et al., Science 314, 439 (2006)

# Cygnus region: diffuse gamma-rays



- Strong & Moskalenko optimized model
  - Increase  $\pi^0$  and IC component throughout Galaxy
  - Milagro 2-6x above prediction (optimized-standard models)
  - Unresolved sources?
  - Cosmic-ray accelerators?

# MGRO J2019+37 field

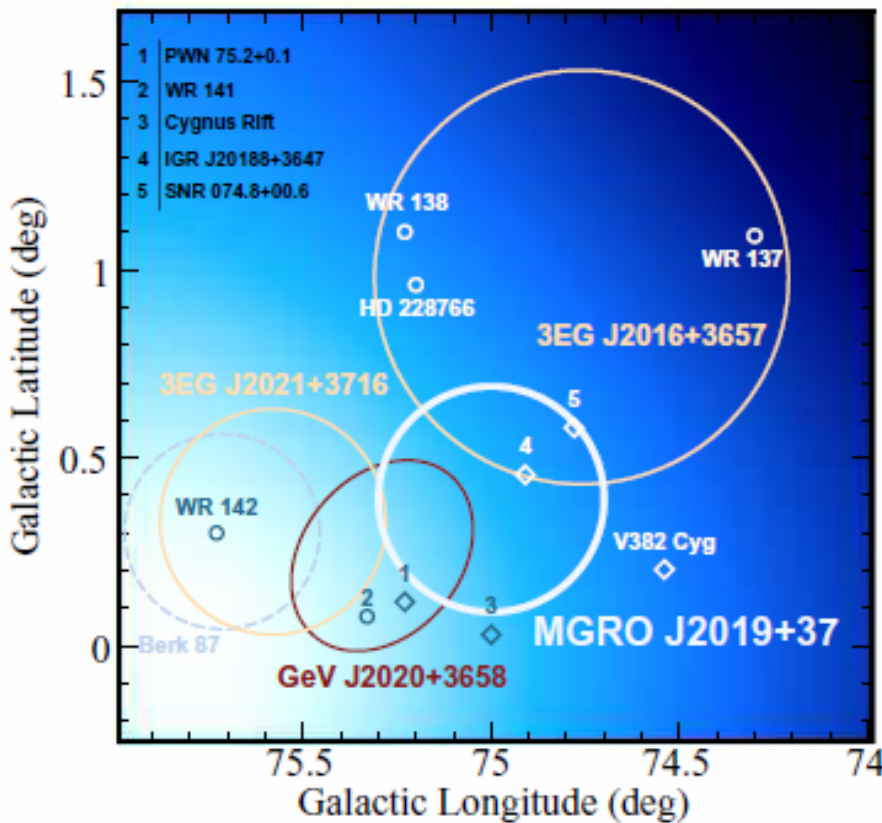


FIG. 1: The field near MGRO J2019+37. Shown are 3EG Catalog sources, a GeV Catalog source, and potential counterparts to the gamma-ray sources. These sources are overlaid upon diffuse GeV emission observed by EGRET (white most intense). For details, please see the caption of Fig. 2.

- 2 EGRET unIDs  
3EG J2016+3657 (blazar?)  
2EG J2021+3716
- GeV J2020+3658 (PWN 75.2+0.1?)
- 5 Wolf-Rayet stars
- 1 Massive eclipsing binary V382 Cyg
- 2 SNRs  
074.8+00.6 (just an H II region?)  
074.9+01.2 (12kpc!)
- IGR J20188+3647 (only in 17-30keV)
- Cygnus rift (molecular cloud complex)

$$r \approx 5 \left( \frac{\theta}{0.3^\circ} \right) \left( \frac{D}{1 \text{ kpc}} \right) \text{ pc}$$
17

# Cygnus region

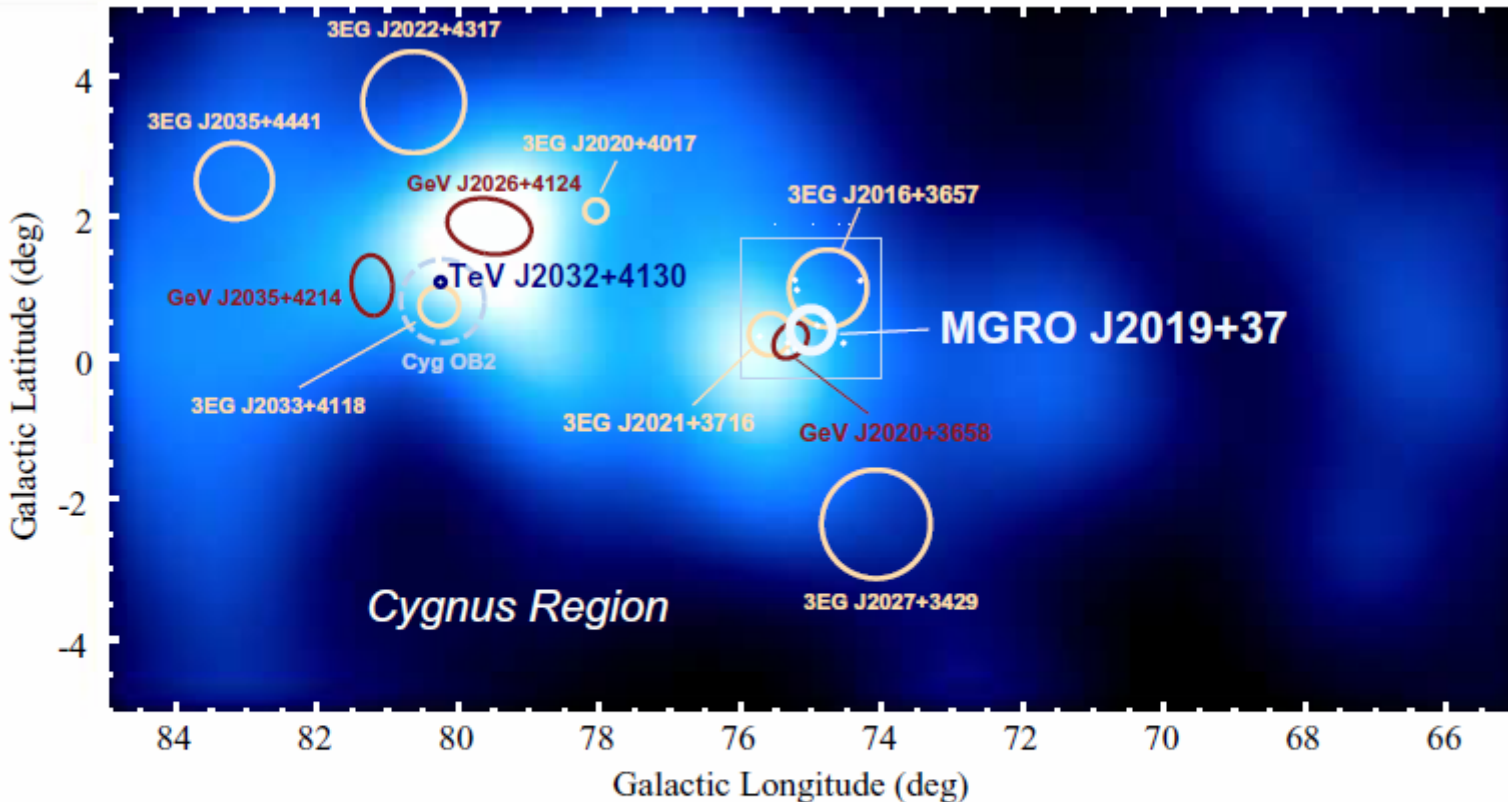


FIG. 2: Gamma-ray sources and diffuse GeV emission in the Cygnus region. Shown are the sources discovered by Milagro (MGRO J2019+37) and HEGRA (TeV J2032+4130), along with their approximate ( $1\sigma$ ) error circles. The fitted extent of the Milagro source is comparable to the circle shown. Also shown are nearby Third EGRET (3EG) (compiled from  $> 100$  MeV gamma rays) and GeV ( $> 1$  GeV gamma rays) catalog sources (all at 95% confidence); as well as gamma-ray source candidates (points), the Cyg OB2 core (dashed circle), and the region of Fig. 18 (box). EGRET 4 – 10 GeV (point-source subtracted) diffuse emission (smoothed and scaled linearly from  $\sim 1 - 10 \times 10^{-6} \text{ cm}^{-2} \text{ s}^{-1} \text{ sr}^{-1}$ , with white most intense) is also displayed.

# Spectral consideration

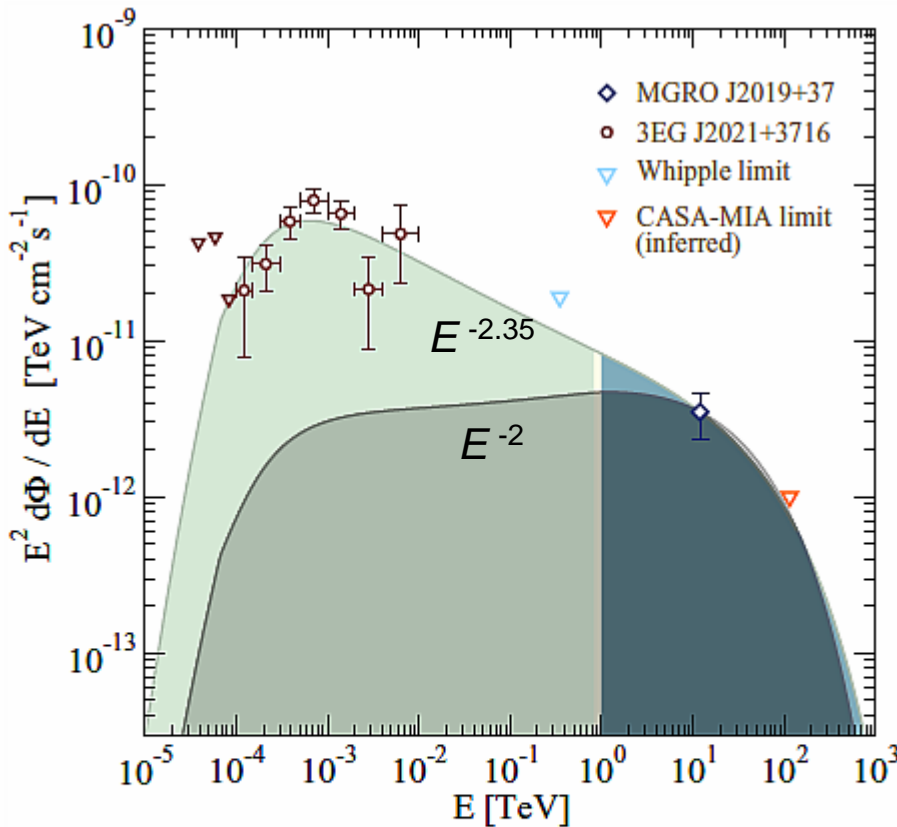


FIG. 3: Data and possible hadronic spectra for MGRO J2019+37. Shown are the Milagro measurement at 12 TeV (diamond), the EGRET spectrum for 3EG J2021+3716 (circles), the upper limit from Whipple (0.3 TeV), and our inferred upper limit from CASA-MIA (115 TeV). Also shown are hadronic fits to the data, assuming  $E_p^{-2.35}$  (upper) and  $E_p^{-2}$  (lower) source proton spectra. The region above 1 TeV is of greatest interest to neutrino astronomy.

## Hadronic scenario

$$dF/dE = E^{-2.35} \exp(-E/E^{\text{cut}})$$

$$E^{\text{cut}} = 1000 \text{ TeV}$$

$$\rightarrow E \approx 5 \times 10^{50} \left( \frac{1 \text{ cm}^{-3}}{n_H} \right) \left( \frac{D}{1 \text{ kpc}} \right)^2 \text{ erg}$$

If a few kpc, this is the order of the total explosion energy of a SN.

$$dF/dE = E^{-2} \exp(-E/E^{\text{cut}})$$

$$E^{\text{cut}} = 500 \text{ TeV}$$

# Neutrino emission

- Neutrino emission from  $p$ - $p$  interaction

$$\pi^+ \rightarrow \mu^+ \nu_\mu \rightarrow e^+ \nu_\mu \bar{\nu}_e \nu_\mu$$

$$\pi^- \rightarrow \mu^- \bar{\nu}_\mu \rightarrow e^- \nu_\mu \bar{\nu}_e \bar{\nu}_\mu$$

- $\nu_e : \nu_\mu : \nu_\tau = 1:2:0 \rightarrow 1:1:1$  by oscillation
- Typical  $\nu$  energy  $\sim \frac{1}{2}$  of  $\pi^0$  gamma-ray
- $d\Phi_\nu/dE_\nu = (1/2)^{\Gamma-1} \phi_\gamma E_\nu^{-\Gamma} = \phi_\nu E_\nu^{-\Gamma}$  (for each  $\nu$ )
- $d\Phi_\gamma/dE_\gamma = A_\gamma E_\gamma^{-\beta} \exp[-(E_\gamma/E_\gamma^{\text{cut}})^{1/2}]$   
where  $\beta=2.2$ ,  $E_\gamma^{\text{cut}}=45\text{TeV}$  for  $E_p^{-2.35}$ ,  
 $\beta=1.9$ ,  $E_\gamma^{\text{cut}}=20\text{TeV}$  for  $E_p^{-2}$

# Neutrino-induced muon spectrum

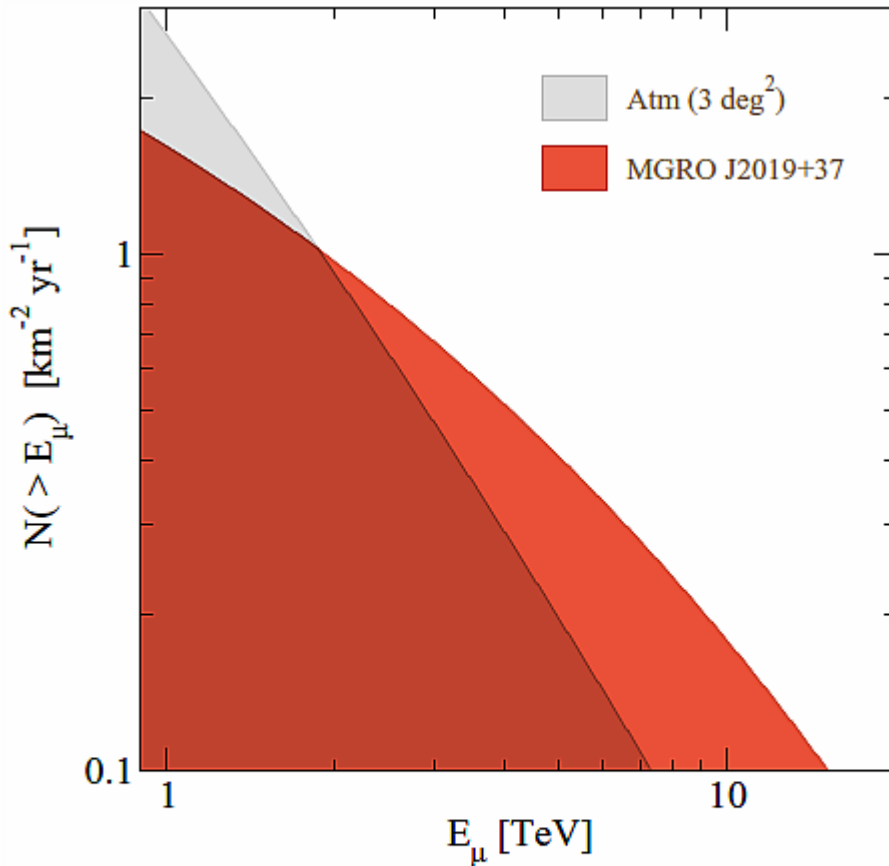


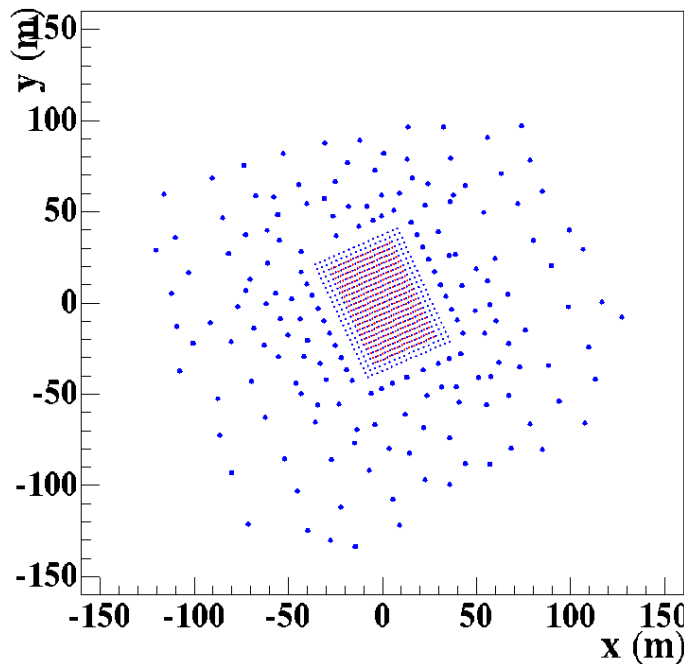
FIG. 4: Integrated ( $\nu_\mu + \bar{\nu}_\mu$ )-induced muon rates from MGRO J2019+37 above a given muon energy within IceCube for one year. These rates result from an  $E_p^{-2.35}$  source proton spectrum (see Fig. 3). The  $E_p^{-2}$  fit yields a nearly identical result. The shaded region shows the expected atmospheric background in a 3 deg<sup>2</sup> bin.

$$\begin{aligned} \nu_\mu + p &\rightarrow \mu^+ + X \\ E_\mu &> 1 \text{ TeV} \end{aligned}$$

Detectable by  
IceCube? –  
marginal!  
  
3deg<sup>2</sup> bin –  
cannot resolve!

# HAWC

**Milagro**



Milagro:

450 PMT (25x18) shallow (1.4m) layer  
 273 PMT (19x13) deep (5.5m) layer  
 175 PMT outriggers

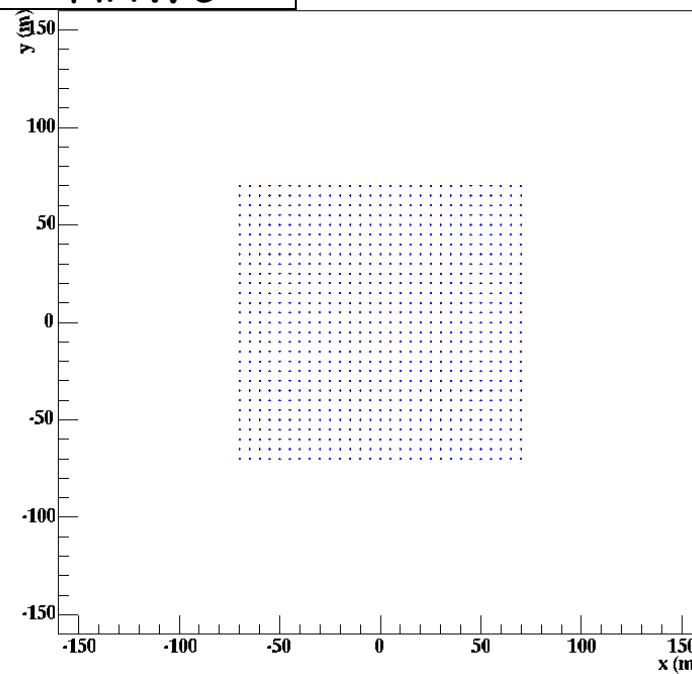
Instrumented Area: ~40,000m<sup>2</sup>

PMT spacing: 2.8m

Total Area: 3500m<sup>2</sup>

$\mu$  det Area: 2200m<sup>2</sup>

**HAWC**



HAWC:

900 PMTs (30x30)  
 5.0m spacing  
 Single layer with 4m depth

Mexico?  
 2010?

Instrumented Area: 22,500m<sup>2</sup>

PMT spacing: 5.0m

Total Area: 22,500m<sup>2</sup>

$\mu$  det Area: 22,500m<sup>2</sup>